

Power Optimization in Nano Sensor Networks for Chemical Reactors

Eisa Zarepour, Mahbub Hassan, Chun Tung Chou
School of Computer Science and Engineering
University of New South Wales, Sydney, Australia
{ezarepour, mahbub, ctchou}@cse.unsw.edu.au

Adesoji A. Adesina*
ATODATECH LLC, Brentwood
CA 94513 USA
ceo@atodatech.com

ABSTRACT

Chemical reactors are designed to efficiently produce high-value chemical products but at the same time they also produce low-value by-products. The selectivity of a chemical process refers to the proportion of high-value product produced. A nano sensor network (NSN) monitoring the chemical process at the molecule level could help improving the selectivity by preventing the reactions that lead to low value by-products. Therefore, a central requirement to achieve high selectivity by NSN is reliable communication. A challenge to realising reliable communication within a chemical reactor is its time-varying chemical composition, which in turn creates a time-varying radio channel and noise. The sensor nodes therefore need to adjust their transmission power according to the chemical composition while maintaining a low overall power budget. We show that this problem can be modelled as a Markov Decision Process (MDP). However, the MDP solution requires the sensors to know the composition of the reactor at each time instance, which is prohibitive. We therefore derive off-line time-based policies that these sensors can use. We illustrate our work by using an important chemical process for fuel production and demonstrate the performance of our proposed off-line policies against the optimal MDP policy.

1. INTRODUCTION

Nanosensors are tiny motes (nanomotes) made from novel nanomaterials capable of sensing new types of phenomenon at the molecular level. For example, a hydrogen nanosensor was reported in [23], where the optical properties of the palladium layer changes when exposed to hydrogen. Yonzon et al. [27] survey many other types of nanosensors that can be used for chemical and biological sensing. Similarly, significant progress has been made in building nanoactuators that can be used to accomplish some basic tasks at

*This work was initiated while the author was with the School of Chemical Engineering at University of New South Wales, Sydney, Australia.

Permission to make digital or hard copies of all or part of this work for personal or classroom use is granted without fee provided that copies are not made or distributed for profit or commercial advantage and that copies bear this notice and the full citation on the first page. Copyrights for components of this work owned by others than ACM must be honored. Abstracting with credit is permitted. To copy otherwise, or republish, to post on servers or to redistribute to lists, requires prior specific permission and/or a fee. Request permissions from Permissions@acm.org. NANOCOM' 14, May 13 - 14 2014, Atlanta, GA, USA.

Copyright 2014 ACM 978-1-4503-2979-8/14/05...\$15.00
<http://dx.doi.org/10.1145/2619955.2619973>.

the molecular level by harnessing the interactions between nanoparticles, electromagnetic fields and heat [3, 6]. The next step is to connect these nanosensors into a wireless nano sensor network (NSN) for wider coverage and control of the environment. NSNs open up the possibility to sense and control important physical processes from the very *bottom*, right at the molecule level. There are early indications suggesting that such *bottom-up* approach to sensing and control, which has hitherto not been possible with conventional macro-scale wireless sensor networks, has the potential to radically improve the performance of many applications in medical, biological, and chemical fields [2, 3, 28, 29].

In our earlier work [28, 29, 30], we have shown how a NSN could be deployed inside a reactor for a bottom-up control of the chemical synthesis with the ultimate goal of improving the performance of the reactor. Chemical reactors are built to produce some high-value products, but they also generate some low-value materials as a by-product of some specific chemical reactions. The performance of a reactor is measured by its *selectivity*, which refers to the percentage of high-value products in the overall output [20]. By monitoring a reactor at the molecular level and turning off elementary reactions leading to undesired molecular species, a NSN can potentially achieve very high selectivity.

An important finding of our earlier work [30] is that the packet loss in the NSN reduces its ability to monitor and control chemical reactions, which ultimately reduces selectivity. The impact of packet loss on the selectivity depends on the chemical composition of the reactor. Interestingly, as nanomotes are expected to operate in the terahertz band [3], the absorption coefficient and the packet error rate (PER) at the receiver are also heavily influenced by the molecular composition of the reactor. However, unlike a home or an office environment, the chemical composition of the reactor varies rapidly due to the chain reactions consuming certain molecules and producing others. The time-varying composition leads to changing absorption coefficients, which in turn leads to changing PER. This means the nanomotes cannot use the same power throughout the chemical production. If the nanomotes choose to use a very high power so that they can overcome the worst possible absorption during the lifetime of the synthesis, this high power creates a high interference when the channel is good. Similarly, the nanomotes cannot choose a low power that is only suitable for good channel condition because the nanomotes will not be able to communicate when the channel is bad. For autonomous NSNs, which are powered by limited-capacity nano-batteries [24, 25] or limited-throughput energy-harvesting circuits [22,

26], a better strategy is to adjust the power over time to maximize the selectivity with a minimal amount of power consumption.

In this paper, we make the following contributions. We show that the optimal power allocation strategy can be obtained by formulating the problem as a Markov Decision Process (MDP). However, the MDP solution requires the nanomotes to know the chemical composition of the reactor at any given time, which is not practical. We, therefore, propose an alternative for the nanomotes to adjust power following a rule or heuristic computed offline. By simulating the process details of a real chemical reactor, we demonstrate that the proposed heuristics perform well relative to MDP optimization.

The rest of the paper is organised as follows. Related work is reviewed in Section 2 followed by a more detailed overview of NSNs for chemical reactors in Section 3. We present our MDP formulation and its solution in Section 4. Section 5 explains the proposed offline power allocation heuristics with numerical results presented in Section 6. We conclude the paper in Section 7.

2. RELATED WORK

Much work has been done in using power allocation to combat the effect of time-varying wireless communication channel due, for example, to fading or node mobility. For example, in [15] the technique of Lyapunov optimization [18] has been extended to perform a joint optimization on routing and power allocation to provide bounded average delay in a wireless network with time-varying channel. Similarly, several attempts have been made to maximize the application layer performance via an optimum power allocation scheme in time-varying wireless sensor networks (WSNs). For instance, the papers [19] and [32] use power allocation to optimize, respectively, the mean squared error and probability of detection, in wireless sensor networks. Although these work, as well as ours, aim at using power allocation to improve the application layer performance, our performance objective is the selectivity of a chemical production process, which is a very different type of performance metric.

A common technique to deal with time-varying channel is to use feedback mechanisms. There are a lot of past work in this field. We would like to highlight the work [5] which takes into account the battery power level of resource constrained device into account. The work therefore targets resource constrained devices. However, it is not sure whether this scheme can be applicable to NSNs due to their extremely constrained resources. Therefore, in this paper, we focus on deriving off-line policies that nanomotes can use without any online feedback from the channel.

There are also a lot of works on designing optimum power allocation for WSNs in a specific topology such as grid or honeycomb structure. In [12] a local power allocation strategy for WSNs has been proposed that operates based on estimation of the distance between sensors. In [14] an adaptive power control scheme for WSN has been introduced that aims to improve the quality of the link between sensors by building a model for each node describing the correlation between transmission power and link quality of each individual neighbour over time. Authors in [13] have proposed a new method based on sleep state policy to optimize power allocation and increase the lifetime of the WSN. A distinguishing feature of our work is that, the nanomotes, due

to their very limited resources, are not able to perform extensive computation. We therefore focus on off-line power allocation algorithms.

There is limited work done on power allocation specifically for wireless NSNs. In a recent work, Jornet and Akyildiz [9] considered optimization of the power spectral density (PSD) of the transmitted signal over the terahertz band. In our work, we use the same molecular noise and path loss model of [9], but instead of optimizing the PSD, we consider dynamic power allocation with the aim of improving packet delivery rate with the ultimate aim of achieving better selectivity.

Work on NSN applications to chemical reactor performance improvement is rare. In [28, 30, 29], we showed how NSN could be potentially deployed on the surface of a reactor catalyst to control and improve selectivity of the reaction process from the bottom up. In [31], we proposed frequency hopping for NSN as a method of mitigating absorption of THz radiation in a chemically changing environment. The current work is different from these previous works in that it aims to maximize selectivity with minimal power consumption in the NSN by dynamically adjusting the transmit power.

3. NSN FOR CHEMICAL REACTORS

Catalysts are often used in chemical reactors to speed up the reaction process. The surface of a catalyst contains numerous *sites* where reactants (molecules) adsorb and react with each other. Only one molecule can be adsorbed in an empty site at any given time and it can only react with a molecule adsorbed in another close-by site. After a reaction between two molecules in two close-by sites, a different molecule is formed in either of the two sites, making one of them empty again. This process continues until all input molecules are used up. Some composite molecules desorb from the sites, which become the (desired or unwanted) output of the reactor. Figure 1 shows a magnified view of a catalyst and a proposed NSN with nanomotes filling up each site. Each nanomote is assumed to be capable of sensing the molecule type adsorbed (or attempting to adsorb) in the site, communicate with other nanomotes in the vicinity, and perform actuation to prevent adsorption of specific molecule types attempting to adsorb in the site.

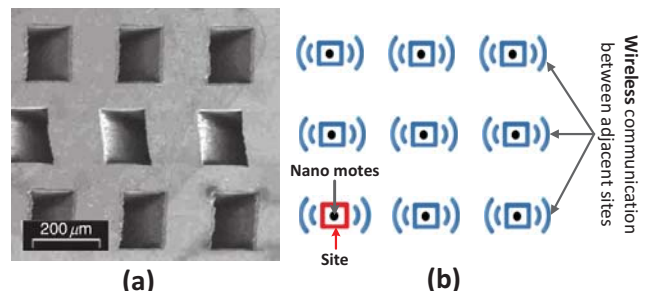


Figure 1: (a) A scanning electron microscopy image (adapted from [17]) showing that the sites are arranged in a regular 2D grid, (b) an imaginary 3x3 nano sensor grid where each site hosts a nanomote.

In order to give a more concrete discussion on how NSN can be used to improve chemical production, we have cho-

sen to use Fischer-Tropsch (FT) synthesis [1] which is a major process for converting natural gas to liquid hydrocarbons. IN FT synthesis, a hydrogen atom H can react with molecules having the chemical formula C_nH_{2n+1} to form paraffins, which is an unwanted product of this synthesis. This class of reactions is known as hydrogen-to-paraffin (HTP) reactions. The aim of the proposed NSN is to suppress the number of HTP (unwanted) reactions by ensuring that there are no hydrogen atoms near the vicinity of a C_nH_{2n+1} so that HTP reactions cannot occur. An example in Figure 2 shows that adsorption of H in Site 1 could lead to paraffin because of the presence of a C_4H_9 in the neighborhood, but its adsorption in Site 2 cannot produce paraffin. Therefore, if the nanomote at Site 1 knows that its neighbouring site has a C_4H_9 , it can attempt to prevent the hydrogen H atom from adsorbing into its site, preventing an HTP reaction and improving the selectivity thereby. In order for all this to work, one important requirement is that nanomotes must be able to communicate with each other reliably. Our previous work shows that selectivity is sensitive to the packet loss in the network [30].

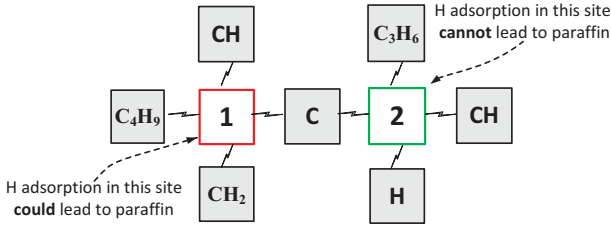


Figure 2: Nano sensing and control on the surface of a catalyst. Nanomote in Site 1 prevents H adsorption, but the nanomote in Site 2 allows it.

4. MDP FOR DYNAMIC POWER ALLOCATION

In Section 3, we describe how a NSN can be used to improve the selectivity of a chemical production by suppressing those undesirable chemical reactions that lead to low value products. We also explain that the efficacy of suppressing the undesirable reactions depends on the PER between neighbouring nodes in the NSN. The PER depends on the transmission power, path loss, molecular absorption noise and interference. The latter three factors depend on the chemical composition of the transmission medium [9], which is constantly changing in a chemical reactor because of production and consumption of chemical molecules. Therefore, if the nanomotes use a constant transmission power, the PER will change over time and this can affect the selectivity. An alternative strategy is for the motes to adjust their transmission power to keep the PER low. However, given the limited energy budget of an autonomous NSN, the transmission power has to be appropriately adjusted to give maximum improvement in selectivity. In this section, we show that this dynamic power allocation problem can be formulated as an MDP.

In section 4.1, we use a simple example to illustrate how an *uncontrolled* chemical reaction can be modelled by an

embedded Markov chain (EMC). The aim of this section is to draw a connection between state transition probability and reaction rates. Given that the goal of our NSN is to control the reaction rates, which is related to the state transition probability, therefore the power allocation problem can be formulated as an MDP. In section 4.2, this MDP will be defined.

4.1 Markov chain for uncontrolled chemical reactions

The paper [8] proves that the dynamics of a set of chemical reactions can be modelled by a continuous-time Markov chain (CTMC). We use a simple example to illustrate the idea. In particular, we want to show how the states and transition probabilities are defined. This will help us to define the MDP problem in the next section. We consider a

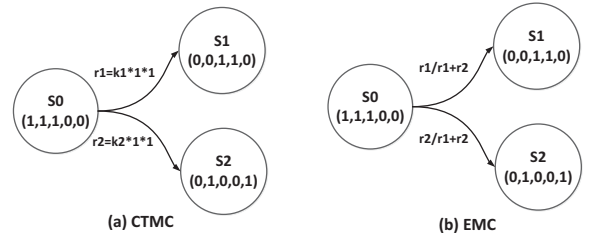


Figure 3: CTMC and EMC of a simple set of chemical reactions.

chemical reactor with 3 input chemical species A , B and C . Two possible chemical reactions can take place in this reactor. In the first reaction, a molecule of A reacts with a molecule of B to form a molecule of D ; this is commonly expressed using the chemical formula of $A + B \rightarrow D$. The second reaction is $A + C \rightarrow E$. We use n_X to denote the number of molecules of chemical species X . The state of the chemical reactor is the 5-tuple $(n_A, n_B, n_C, n_D, n_E)$. That is, the state consists of the number of each type of molecules in the chemical reactor. For simplicity, we assume the initial state of the reactor is $S_0 = (1, 1, 1, 0, 0)$ which means there is a molecule of A , B and C and no molecules of D and E . If the reaction $A + B \rightarrow D$ occurs, then the state will transit from S_0 to $S_1 = (0, 0, 1, 1, 0)$ with one molecule of C and D . Similarly, if $A + C \rightarrow E$ occurs, then the state will become $S_2 = (0, 1, 0, 0, 1)$. Given the initial state S_0 , it can be seen that S_0 , S_1 and S_2 are all the allowable states. These are the states of the CTMC, see figure 3(a). The transition rate of the CTMC is governed by the rate of chemical reactions. For reaction $A + B \rightarrow D$, the reaction rate is $r_1 = k_1 n_A n_B$ where k_1 is the kinetic constant of this reaction and a larger k_1 means a higher likelihood for the reaction to occur (= high state transition rate). Note also that the reaction rate depends on the state. The transition rate from S_0 to S_1 is r_1 . Similarly, the transition rate from S_0 to S_2 is $r_2 = k_2 n_A n_C$. The CTMC is now completely defined and is illustrated in figure 3(a). In order to leverage the theory of MDP to solve the power allocation problem, we convert the CTMC to an Embedded Markov Chain (EMC) [21]. Figure 3(b) illustrates the EMC of the CTMC in figure 3(a). The states of the EMC are the same as those of CTMC. However, the transition rates have been replaced by transition probability. In particular, for our example,

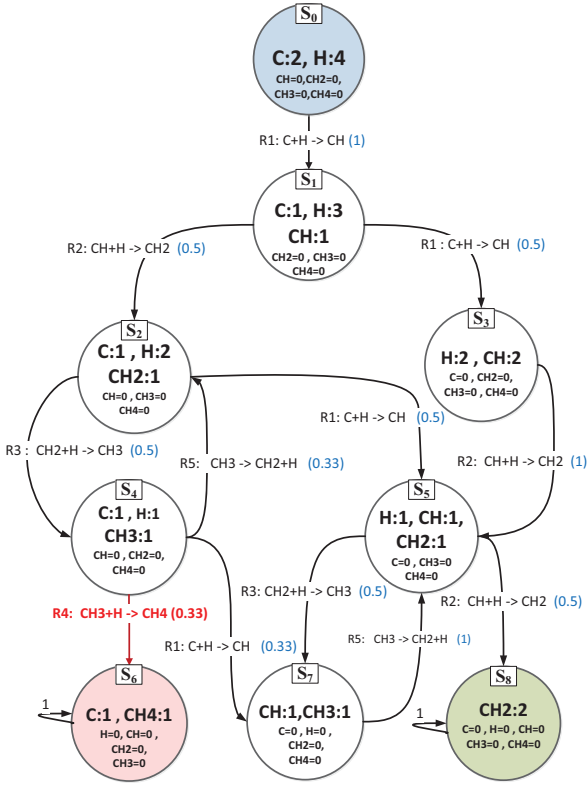


Figure 4: EMC for the FT process with an initial state of 2 carbon and 4 hydrogen atoms. S6 and S8 are absorbing states. The blue number in the parentheses are probability of transition from one state to another state. NSN aims to reduce the rate of HTP reactions e.g. in this example the NSN tries to reduce probability of going from state 4 to state 6.

the transition probabilities from S_0 to, respectively, S_1 and S_2 , are, $\frac{r_1}{r_1+r_2}$ and $\frac{r_2}{r_1+r_2}$. In general, if the transition rate from state S_i to S_j in a CTMC is q_{ij} , then the transition probability from state S_i to S_j in the corresponding EMC is $\frac{q_{ij}}{\sum_j q_{ij}}$ if $i \neq j$ and is zero otherwise.

4.2 MDP formulation

We now present an MDP formulation for the dynamic power allocation problem for the FT reactions.

4.2.1 States

The state of the FT process consists of the number of each type of molecules in the FT process. For illustration, Figure 4 shows the EMC for the *uncontrolled* FT process where the initial state S_0 consists of 2 carbon (C) and 4 hydrogen (H) atoms. The process consists of altogether 9 different states with different chemical compositions in each state. The transition probability of the EMC has been calculated from the corresponding CTMC using the method described earlier.

The states S_6 and S_8 of the EMC are the absorbing states. When the FT process reaches any one of its absorbing states, we assume the chemical production is complete. The chem-

ical composition of the absorbing state is important. If an absorbing state consists of a larger quantity of high value product, then the selectivity of that state is high.

4.2.2 Actions

We assume that at each state, m different transmission power levels P_1, P_2, \dots, P_m are available for the nanomotes to use. The actions of the MDP are these different power levels. This can be viewed as a cross-layer optimisation where physical layer parameter (in our case, power) is used to maximise selectivity, which is an application layer performance.

We will use the EMC in figure 4 to explain the effect of the actions. Our discussion focuses on state S_4 . This state can transit to states S_2, S_6 and S_7 . The probability of transiting to each of these states in the (uncontrolled) EMC is the same ($=0.33$). This also means that the transition rates from S_4 to any one of these states in the corresponding CTMC is the same and we will denote it by r . Out of these three transitions, the move from S_4 to S_6 produces a molecule of CH_4 , which is a low value paraffin. The aim of the NSN is to suppress this reaction as much as possible. Let us assume that the probability of successfully suppressing this reaction by the NSN is p , then NSN reduces the transition rate from S_4 to S_6 from r to $(1-p)r$. The reaction rates from S_4 to states S_2 and S_7 will not be altered by the NSN because no undesirable products are produced. With the revised reaction rate due to the actions of NSN, the transition probability from S_4 to S_6 reduces from 0.33 to $\frac{1-p}{3-p}$ in the (controlled) EMC. This shows how the *probability of successful suppression* affects the state transition probability.

The probability of successful suppression p depends on many factors, including those related to efficiency of sensors and actuators. In this paper, we assume that p is the same as the probability that sensors from neighbouring sites are able to successfully communicate with each other. Hence p is a function of the transmission power, which are the actions of the MDP. At the same time p depends on molecular absorption, which is a function of the chemical composition. Recalling that each state of the MDP is defined by the chemical composition, therefore p is state dependent. Finally, p is also affected by interference due to other nanomotes' transmissions. This interference depends on nanomotes' transmission power and also the composition. To sum up, a chosen transmission power at a given state will give rise to a certain PER, which can in turn affect selectivity.

For the MDP for dynamic power allocation, the actions are the m different power levels. For each power level, we can compute the resulting state transition probability in the EMC similar to that described earlier. Note that the calculation takes into account the transmission power and channel condition, which is state dependent.

4.2.3 Revenue function

The revenue is a function of two quantities, the rate of HTP reactions (r), and the power level (P_i) chosen, where $r > 0$ and P_i is within the range 10^{-16} to 10^{-11} . Increasing r and P_i should have a negative effect on revenue (or selectivity), and vice versa. This can be captured via different types of functions. Because P_i has a wide range, we define the function as:

$$Revenue = \frac{1}{r} + \frac{1}{\log(P_i)}$$

4.3 Large scale MDP

The number of states in the FT process increases exponentially with the number of initial atoms. For example, for the initial gas feed comprising only 10 carbon and 20 hydrogen atoms, we obtain in excess of 35,000 states. For a feed gas with large number of carbon and hydrogen atoms, we face a state explosion problem, which makes it difficult to solve the MDP problem and obtain the optimum policy within a reasonable time.

There are several attempts in the literature to alleviate the MDP state explosion by techniques such as state space reduction and other approximation methods. Kearns et al. [11] proposed a *sparse sampling algorithm* which yields a near-optimal outcome for a large or infinite MDP. In order to implement this algorithm in our context, we start with an initial state with a given number of carbon and hydrogen atoms and then as long as an absorbing state has not been reached, the following steps are executed for each state S_i reached:

1. Calculate the revenue for all possible actions (power levels)
2. Select the action with maximum revenue and call it P_{opt_i} .
3. Use the state transition probabilities for action P_{opt_i} to randomly follow one of these state transitions and move to the next state based on the selected transition. Go back to 1 if the new state is not absorbing.

Note, that the algorithm does not attempt to solve the MDP problem, i.e., it does not attempt to find an (optimum) action for every possible state. Instead, it produces a trace of states and associated power levels from the initial state to the absorbing state, which is then used to derive selectivity and average power level.

5. LOCAL POWER ALLOCATION POLICIES

MDP provides the optimal power allocation policy, but requires the nanomotes to know the *global* state, or the exact chemical composition, of the chemical reactor. This is not a practical policy because it requires each nanomotes to broadcast its local state in the NSN, which would consume a lot of energy. In this section, we investigate the possibility of each nanomote executing the same local pre-planned (or open loop) policy where the transmission power is adjusted over time. A pre-planned policy can be expressed as a univariate function $t \mapsto P(t)$ where $P(t)$ specifies the power level that the nanomotes should use at time t . We propose three heuristics to derive pre-planned policies.

5.1 Local policy based on reaction rates

Since the goal of the NSN is to reduce the number of HTP reactions (the undesirable reactions) in the FT reactor, a possible policy is for the nanomotes to reserve the transmission power when the HTP reactions are more likely to occur so as to increase the chance of suppressing them. To verify the validity of this policy, we first check whether there is a correlation between high transmission power from the MDP solution and high HTP reaction rates. Figure 5 shows a scatter plot of optimal power allocated by MDP and the ratio of HTP reactions to all other reactions taking place in the reactor for one of the sample paths. We find that MDP

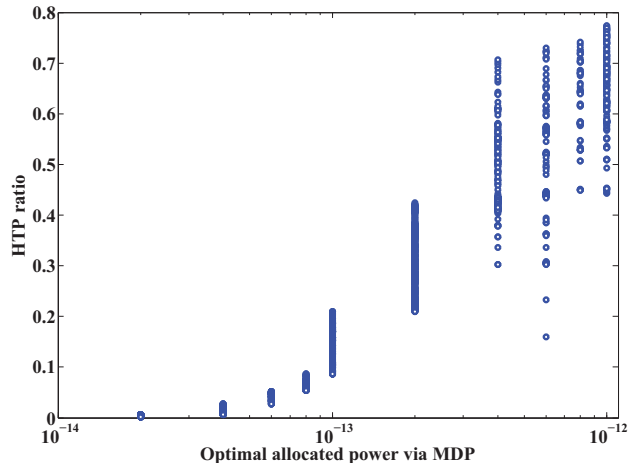


Figure 5: The correlation between HTP reaction rate and the optimal power allocated by MDP.

allocates higher powers when HTP reactions are happening more frequently, and vice versa. The same observation also applies to other sample paths.

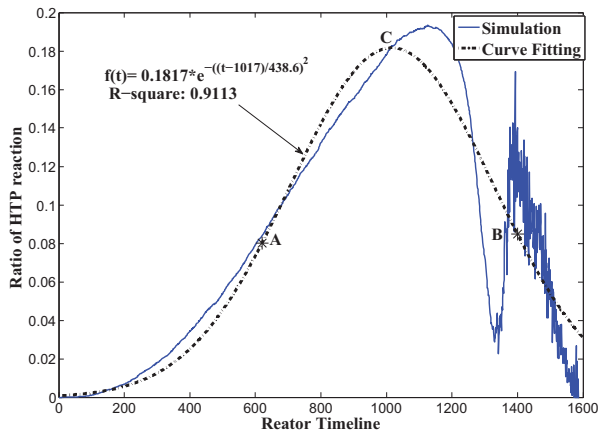


Figure 6: The thick line shows the fraction of HTP reactions at a given time based on the average of 50 SSA simulations. The thin line is a curve fit with an exponential function.

The methodology for building a reaction rate based policy is best explained by an example; however, note that the methodology is general and can be generalised to other chemical reactors. Consider an *uncontrolled* FT process whose initial state has 500 carbon and 1200 hydrogen atoms. We use the stochastic simulation algorithm (SSA) [7], which is a standard algorithm to simulate Markov chain for chemical reactions. We perform 50 simulation runs and compute $\rho(t)$ which is the ratio of the total rate of HTP reactions at time t to the total rate of all reactions at time t . By definition, $\rho(t) \in [0, 1]$ and a higher $\rho(t)$ means a higher probability that an HTP reaction will take place at time t of the *uncontrolled* FT process. We average the 50 $\rho(t)$

curves from 50 simulations to obtain the average curve $\bar{\rho}(t)$. We plot $\bar{\rho}(t)$ in figure 6. The curve $\bar{\rho}(t)$ increases initially as HTP reactions occur through the consumption of the initial supply of H in the gas feed, but starts to fall off after about 1200 in the reactor timeline as the initial H supply runs out. We observe that the $\bar{\rho}(t)$ -curve becomes rather oscillatory towards the end of the synthesis. In order to obtain a policy which is smooth over time, we fit a smooth curve $\bar{\rho}_s(t)$ to $\bar{\rho}(t)$, see figure 6. The rationale of the reaction rate-based policy is to choose the transmission power level at time t to be proportional to $\bar{\rho}_s(t)$ so that a higher power is used when the chance of an HTP reaction occurring is high. We assume that the nanomotes use m discrete power levels with $P_1 < P_2 < \dots < P_m$. We compute $\hat{P}_{RR}(t) = P_m \frac{\bar{\rho}_s(t)}{\max_t \bar{\rho}_s(t)}$ which means $\hat{P}_{RR}(t)$ is P_m at the time instance that $\bar{\rho}_s(t)$ is maximised. For each t , we map $\hat{P}_{RR}(t)$ to the closest value in $\{P_1, P_2, \dots, P_m\}$ to obtain the power level to be used. We will refer to this as the reaction rate-based local policy (RRLP).

5.2 Local policy based on noise distribution

A problem with RRLP is that it does not take the noise into consideration. The noise in the FT process varies over time due to the changing composition in the reactor. For example, at points A and B in figure 6, RRLP uses the same power level because the mean fractions of HTP reactions are the same at these two points in time. However, the chemical composition in the reactor at these two points are different and it results in different amount of noise levels. In fact, the noise level at point A is much lower than that at point B . A noise base policy would therefore allocate a higher transmission power to point B in order to compensate for the noise. We now explain how a local policy based on noise levels can be developed.

The methodology for developing a noise based policy is similar to that of reaction rate based policy. For a given initial composition, we use the SSA to simulate the CTMC of the *uncontrolled* FT process. At each time t , we record the state of the CTMC which is the chemical composition in the reactor at time t . Given this composition at time t , we use the algorithm in [16] to compute the level of molecular absorption noise at time t . We repeat the simulation a number of times and compute the average molecular absorption noise $\bar{n}(t)$ at time t . Figure 7 shows the $\bar{n}(t)$ curve from the average of 50 simulation runs of the FT process with 500 carbon and 1200 hydrogen atoms initially. The figure shows that the noise level increases rapidly as the FT reactions progress. The noise level near the end of the FT process is about an order of magnitude higher than that initially. Since $\bar{n}(t)$ has some high frequency fluctuations near the end of the reaction run, we approximate $\bar{n}(t)$ by an exponential function $\bar{n}_s(t) = 2.73 \times 10^{-15} \times e^{(0.003913t)}$ to smooth out the fluctuations. The rationale of the noise-based policy is to use a higher transmission power when the noise is higher. We compute $\hat{P}_n(t) = P_m \frac{\bar{n}_s(t)}{\max_t \bar{n}_s(t)}$. For each t , we map $\hat{P}_n(t)$ to the closest value in $\{P_1, P_2, \dots, P_m\}$ to obtain the power level to be used. We will refer to this as noise-based local policy (NLP).

5.3 A local policy based on reaction rate and noise

RRLP allocates higher transmission power when the HTP

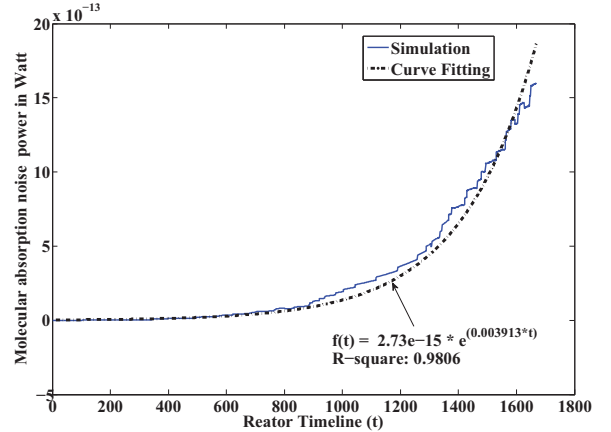


Figure 7: Molecular noise is fitted as an exponential function of time.

reaction rate is high while NLP allocates higher power when the noise is high. If we compare figures 6 and 7, we see that during the third quarter of the reaction cycle, reaction rate is high while noise is low, but during the last quarter, the reaction rate is low but noise is high. This means that RRLP may not perform well in the last quarter and NLP not performing well in the third quarter. To overcome this problem, we propose a local policy that uses both reaction rates and noise levels. The rationale of this local policy is to use high transmission power when *either* reaction rate *or* noise is high.

To describe this policy, we assume that we have already computed $\bar{\rho}_s(t)$ and $\bar{n}_s(t)$ as before. We define the function as:

$$\hat{P}_{RR,n}(t) = P_m \max \left(\frac{\bar{\rho}_s(t)}{\max_t \bar{\rho}_s(t)}, \frac{\bar{n}_s(t)}{\max_t \bar{n}_s(t)} \right) \quad (1)$$

The use of the max function will ensure that $\hat{P}_{RR,n}(t)$ is large when either $\bar{\rho}_s(t)$ or $\bar{n}_s(t)$ is big. The final step is to map $\hat{P}_{RR,n}(t)$ to the closest value in $\{P_1, P_2, \dots, P_m\}$. We will refer to this policy to as reaction-rate and noise local policy (RR+NLP).

6. RESULTS

This section aims to study the performance of the local policies proposed in section 5. A good policy is one which produces a higher selectivity for a given power budget. We compare these local policies against the the MDP policy and constant power allocation.

Methodology

We assume the FT process starts with 500 carbon and 1200 hydrogen atoms. The chemical production continues until no more new chemicals can be produced. The distance between two neighbouring nanomotes is assumed to be 1 μm . The reactor is assumed to operate at a temperature of 500K and pressure of 10 atmospheres. We follow the procedure of [16] to compute the molecular absorption noise/attenuation and PER. As in [16], we assume each pulse has a duration of 100 fs and the spectrum band is 0.1–10 THz. The molecular absorption noise in the reactor depends on the chemical composition within the reactor and we need the molecu-

lar absorption coefficient of the chemical species within the reactor. This information is obtained from the HITRAN database [4]. The nanomotes use ON-OFF keying [10] where a pulse is sent for a bit 1. We assume the probabilities of bit 1 and bit 0 are equal. To model the interference between different nanomotes, we assume each nanomote transmits with a certain probability and compute the total interference power at the nanomotes. We then compute the PER using the signal-to-interference-noise ratio.

We conduct 30 sets of experiments, each with a different nominal power level P_{nominal} chosen from 10^{-16} to 10^{-11} W. The schemes to be compared are constant power allocation, MDP and the three local policies (RRLP, NLP, RR+NLP) proposed in the previous section. We now explain how these schemes make use the the nominal power level.

For constant power allocation, each nanomote uses P_{nominal} as the transmission power. For other policies, we generate m discrete power levels. The minimum power P_1 is zero which means the nanomotes do not communicate. The other $m - 1$ power levels are drawn from $[\frac{P_{\text{nominal}}}{100}, 100P_{\text{nominal}}]$ with maximum power $P_m = 100P_{\text{nominal}}$ and that have been equally spaced in this range. These m power levels are used by the MDP and the three local policies. Here, we use $m = 11$.

For MDP, we use the sparse sampling method to compute selectivity and average power usage. For constant power allocation and local policies, we incorporate the power selection into the transition rates of the CTMC describing the FT process. We can therefore simulate these by using SSA. At the end of each simulation, we compute the selectivity and the *average* power usage for that simulation run. Note that the *average* power usage for MDP and the local policies can be *different* from the nominal power. For each of these policies, we repeat the simulations five times and then average the results over the five simulation runs to obtain the final results.

Results and discussions

Figure 8 shows the power-selectivity tradeoff for the constant power allocation, MDP and the three local policies. As a reference, we have also shown the average selectivity for the uncontrolled FT process in the figure. The figure shows that all the four power allocation schemes achieve better selectivity than the uncontrolled FT process. As expected, the MDP solution (optimal policy) gives the highest selectivity for a given power budget and outperforms all the other schemes. For power budget below 2×10^{-14} W, the MDP and all the three local policies give similar results. For higher power budgets, RR+NLP is the best performing local policy. We also notice that for higher power, the proposed local policies perform much worse than the optimal policy. We leave the design of better approximations that can match the optimal solution as a future work.

Figure 9 shows typical policies (power-time function) for MDP, RRLP, NLP and RR+NLP. All these policies consume a total power of around 1.5×10^{-13} W and is the average of 2 simulation runs. The RRLP policy results in a selectivity of 0.46 and puts most of its power in the middle of the reaction process cycle. The NLP policy has a selectivity of 0.59 and puts most of its power near the end. Neither of them produces very good result. The RR+NLP has the best performance out of the three local policies. It allocates its power at where HTP reaction rates or noise is high. It results in a higher selectivity of 0.71 compared with the other

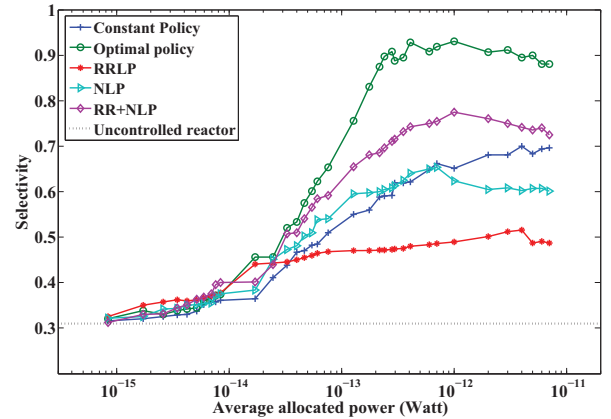


Figure 8: The selectivity achieved by different power allocation policies for a given power budget.

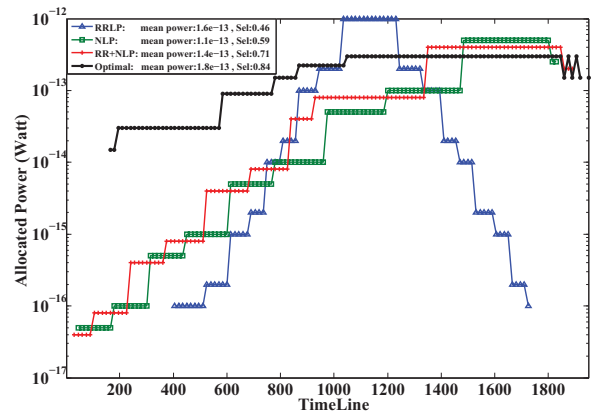


Figure 9: Typical policies for MDP, RRLP, NLP and RR+NLP.

Policy	Selectivity improvement [%]	Power saving [%]
Optimal	122.5	69.4
RRLP	48.5	10
NLP	71.4	19.6
RR+NLP	93.6	61.6
Constant	71.9	—

Table 1: Selectivity improvements are against the uncontrolled FT process and the power savings are against the constant power allocation.

policies.

In Table 1, we compare the performance of five power allocation policies over a range of nominal power from 10^{-16} to 10^{-11} . If we average the selectivity of each policy over all power budgets, we obtain an average improvement of selectivity for each power allocation policy. The second column of Table 1 shows the selectivity improvement as a percentage using the selectivity of the uncontrolled FT process as the reference. It can be seen that RR+NLP performs better than the other two local policies. However, there is a performance gap of about 30% between the optimal MDP policy and that of RR+NLP. We hypothesise that this is due to the fact that we use the *uncontrolled* reaction rate and noise levels to derive our local policies. Since the aim of the NSN is to control the reactions, the actual state trajectory when the reactor is controlled is different from that of the *uncontrolled* state trajectory. We plan to investigate this problem further.

The performance of the power allocation policies can also be measured by the reduction in power for a given level of selectivity. The third column of table 1 compares the performance of the optimal and local policies with respect to the constant power allocation policy. For that, we divide selectivity to 7 ranges ($0.3 - 0.4, \dots, 0.9 - 1$) and compare the average power consumption of each policy in each range. The average power saving over all selectivity ranges has been presented in the last column of Table 1. The optimal policy saves 69% of the power while RR+NLP saves 61.6%, which is close to that of the optimal policy.

We now turn to study the robustness of the local policies. When we design the local policies, we assume that the initial composition (which will be referred to as the nominal initial composition) is given. In the above performance study, we assume that the initial composition of the reactor is the nominal initial composition. However, it may not be possible to control the operating initial composition in a reactor precisely. Here, we study the performance of the local policies when the operating initial composition in the reactor is different from the nominal initial composition. The nominal initial composition used for design is 500 carbon and 1200 hydrogen atoms. In this study, we use two perturbed operating initial compositions: 450 carbon and 1080 hydrogen atoms (-10% deviation) and 550 carbon and 1320 hydrogen atoms ($+10\%$ deviation). We plot the results on selectivity versus power in figure 10 for RR+NLP. The figure shows the results for MDP, and RR+NLP under the nominal initial composition, as well as under the two perturbed operating initial compositions. It can be seen from the figure that the performance of RR+NLP is robust. Our results, reveal similar robustness for RR and NLP policies.

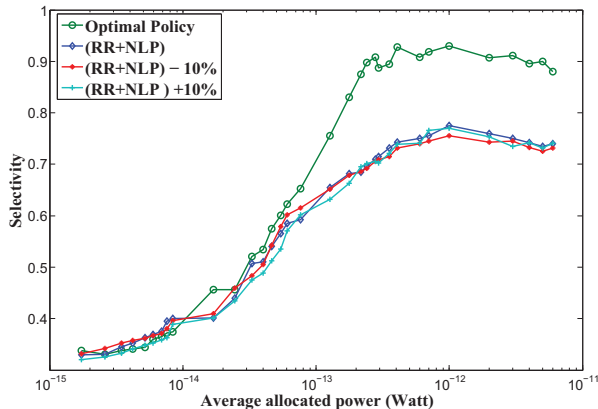


Figure 10: Selectivity versus power for MDP and RR+NLP under nominal initial condition, and the two perturbed operating initial conditions.

7. CONCLUSIONS

NSN can be used to improve the selectivity of chemical synthesis by reducing the production rate of unwanted species. The success of this application requires that the nanomotes be able to reliably communicate with each other. The changing chemical composition within a chemical reactor means that the nanomotes need to adjust their transmission power to maintain reliable communication. We show that an optimal power allocation policy can be derived by using MDP. However, the optimal policy requires the nanomotes to know the exact state of the reactor at any time and this is prohibitive. We therefore study offline policies that do not require nanomotes to know the exact reactor state. We show that these offline algorithms can improve the selectivity of chemical production.

8. ACKNOWLEDGMENTS

Authors acknowledge the use of Leonardi High Performance Computing resource in the Faculty of Engineering, University of New South Wales for this work.

9. REFERENCES

- [1] A. Adesina. Hydrocarbon synthesis via Fischer-Tropsch reaction: travails and triumphs. *Applied Catalysis A: General*, 138(2):345–367, 1996.
- [2] I. F. Akyildiz, F. Brunetti, and C. Blázquez. Nanonetworks: A new communication paradigm. *Computer Networks*, 52(12):2260–2279, Aug. 2008.
- [3] I. F. Akyildiz and J. M. Jornet. Electromagnetic wireless nanosensor networks. *Nano Communication Networks*, 1(1):3–19, Mar. 2010.
- [4] Y. L. Babikov, I. E. Gordon, and S. N. Mikhailenko. "HITRAN on the Web", a new tool for HITRAN spectroscopic data manipulation. In *the proceeding of the ASA-HITRAN Conference*, Reims, France, Aug 29-31, 2012.
- [5] N. Buchbinder, L. Lewin-Eytan, I. Menache, J. Naor, and A. Orda. Dynamic Power Allocation Under Arbitrary Varying Channels; An Online Approach.

- IEEE/ACM Transactions on Networking*, 20(2):477–487, Apr. 2012.
- [6] C. Falconi, a. Damico, and Z. Wang. Wireless Joule nanoheaters. *Sensors and Actuators*, 127(1):54–62, Oct. 2007.
- [7] D. Gillespie. Exact stochastic simulation of coupled chemical reactions. *The journal of physical chemistry*, 81(25):2340–2361, Dec. 1977.
- [8] D. Gillespie. A rigorous derivation of the chemical master equation. *Physica A: Statistical Mechanics and its Applications*, 188:404–425, Sept. 1992.
- [9] J. Jornet and I. Akyildiz. Channel modeling and capacity analysis for electromagnetic wireless nanonetworks in the terahertz band. *IEEE Transactions on Wireless Communications*, 10(10):3211–3221, Oct. 2011.
- [10] J. Jornet and I. F. Akyildiz. Information capacity of pulse-based Wireless Nanosensor Networks. In *the proceeding of the 8th IEEE Communications Society Conference on Sensor, Mesh and Ad Hoc Communications and Networks*, pages 80–88, Salt Lake City, UT, June 27–30, 2011.
- [11] M. Kearns, Y. Mansour, and A. Ng. A sparse sampling algorithm for near-optimal planning in large Markov decision processes. *Machine Learning*, 49:193–208, Dec. 2002.
- [12] W.-H. Liao, K.-P. Shih, and Y.-C. Lee. A localization protocol with adaptive power control in wireless sensor networks. *Computer Communications*, 31(10):2496–2504, June 2008.
- [13] C. Lin, N. Xiong, J. H. Park, and T.-h. Kim. Dynamic power management in new architecture of wireless sensor networks. *International Journal of communication systems*, 22(6):671–693, June 2009.
- [14] S. Lin, J. Zhang, G. Zhou, and L. Gu. ATPC: adaptive transmission power control for wireless sensor networks. In *the proceedings of the ACM Conference on Embedded Networked Sensor Systems (SenSys)*, pages 223–236, Colorado, USA, Nov 1–3, 2006.
- [15] M. Neely, E. Modiano, and C. Rohrs. Dynamic power allocation and routing for time-varying wireless networks. *IEEE Journal on selected areas in communications*, 23(1):89–103, Jan. 2005.
- [16] J. C. Pujol. Bridging PHY and MAC Layers in Wireless Electromagnetic Nanonetworks. *A Final Year Project from Technical University of Catalonia, Spain*, Dec. 2010.
- [17] A. Renken and L. Kiwi-Minsker. Microstructured catalytic reactors. *Advances in Catalysis*, 53(10):47–122, 2010.
- [18] L. Tassiulas and A. Ephremides. Stability properties of constrained queueing systems and scheduling policies for maximum throughput in multihop radio networks. *IEEE Transactions on automatic control*, 37(12), Sept. 1992.
- [19] G. Thattai and U. Mitra. Sensor Selection and Power Allocation for Distributed Estimation in Sensor Networks: Beyond the Star Topology. *IEEE Transactions on Signal Processing*, 56(7):2649–2661, July 2008.
- [20] G. P. Van Der Laan and a. a. C. M. Beenackers. Kinetics and Selectivity of the Fischer-Tropsch Synthesis: A Literature Review. *Catalysis Reviews*, 41(3-4):255–318, Jan. 1999.
- [21] P. Van Mieghem. *Performance Analysis of Communications Networks and Systems*. Cambridge University Press, 2009.
- [22] R. Venkatasubramanian. Energy harvesting for electronics with thermoelectric devices using nanoscale materials. In *the proceeding of IEDM 2007, IEEE Electron Devices Meeting*, pages 367–370, Washington DC, Dec 10–12, 2007.
- [23] J. Villatoro and D. Monzón-Hernández. Fast detection of hydrogen with nano fiber tapers coated with ultra thin palladium layers. *Optics express*, 13(13):5087–92, June 2005.
- [24] F. Vullum and D. Teeters. Investigation of lithium battery nanoelectrode arrays and their component nanobatteries. *Journal of Power Sources*, 146(1-2):804–808, Aug. 2005.
- [25] F. Vullum, D. Teeters, A. Nyten, and J. Thomas. Characterization of lithium nanobatteries and lithium battery nanoelectrode arrays that benefit from nanostructure and molecular self-assembly. *Solid State Ionics*, 177(26-32):2833–2838, Oct. 2006.
- [26] Z. L. Wang. Energy harvesting for self-powered nanosystems. *Nano Research*, 1(1):1–8, July 2008.
- [27] C. R. Yonzon, D. a. Stuart, X. Zhang, and A. D. McFarland. Towards advanced chemical and biological nanosensors—An overview. *Talanta*, 67(3):438–48, 2005.
- [28] E. Zarepour, A. A. Adesina, M. Hassan, and C. T. Chou. Nano Sensor Networks for Tailored Operation of Highly Efficient Gas-To-Liquid Fuels Catalysts. In *Australasian Chemical Engineering Conference*, Brisbane, Australia, 29 Sep - 2 Oct, 2013.
- [29] E. Zarepour, A. A. Adesina, M. Hassan, and C. T. Chou. An innovative approach to improving gas-to-liquid fuels catalysis via nano-sensor network modulation. *Industrial and Engineering Chemistry Research (In Press)*, 2014.
- [30] E. Zarepour, M. Hassan, C. T. Chou, and A. A. Adesina. Nano-scale Sensor Networks for Chemical Catalysis. In *IEEE International Conference on Nanotechnology*, pages 61–66, Beijing, China, Aug 5–8, 2013.
- [31] E. Zarepour, M. Hassan, C. T. Chou, and A. A. Adesina. Frequency Hopping Strategies for Improving Terahertz Sensor Network Performance over Composition Varying Channels. In *IEEE WoWMoM*, Sydney, Australia, 2014.
- [32] X. Zhang, H. V. Poor, and M. Chiang. Optimal Power Allocation for Distributed Detection Over MIMO Channels in Wireless Sensor Networks. *IEEE Transactions on Signal Processing*, 56(9):4124–4140, Sept. 2008.